International Journal of Multidisciplinary Research and Development
Online ISSN: 2349-4182, Print ISSN: 2349-5979
Impact Factor: RJIF 5.72
www.allsubjectjournal.com
Volume 4; Issue 12; December 2017; Page No. 66-73

Molecular structure, NBO analysis, first-hyperpolarizability, and HOMO-LUMO studies of bis(dithiolylidene)-tetrathiapentalene(BDT-TTP) by quantum computational calculations

[*1] Tahar Abbaz, [2] Amel Bendjeddou, [3] Hanane Tabbi, [4] Didier Villemin
[1-3] Laboratory of Aquatic and Terrestrial Ecosystems, Org. and Bioorg. Chem. Group, University of Mohamed-Cherif Messaadia, Souk Ahras, Algeria
[4] Laboratory of Molecular and Thio-Organic Chemistry, UMR CNRS 6507, INC3M, FR 3038, Labex EMC3, ensicaen & University of Caen, Caen 14050, France

Abstract
Optimized molecular structure has been investigated by DFT/B3LYP method combined with 6-31G(d,p) basis set. Stability of the molecule arises from hyperconjugative interactions, charge delocalization and intramolecular hydrogen bond has been analyzed using natural bond orbital (NBO) and nonlinear optical (NLO) analysis. Electronic structures were discussed and the descriptions of frontier molecular orbitals and the relocation of the electron density were determined. E_{HOMO}, E_{LUMO}, energy gap, dipole moment (μ), global hardness (η), softness (S), electrophilicity index (ω), molecular polarizability (α), Mulliken electronegativity (ϰ), and molecular electrostatic potential (MEP) have employed to determine the reactivity of (BDT-TTP) and its derivatives.

Keywords: tetrathiafulvalenes; density functional theory; computational chemistry; electronic structure; quantum chemical calculations

1. Introduction
During the last decades, a great amount of efforts have been devoted to the syntheses and coordination chemistry of organic ligands containing the redox-active tetrathiafulvalene (TTF) unit due to their unique π-electron-donor properties and capability of serving as useful building blocks for new molecular materials [1, 2]. One of the research trends in new TTF derivatives for functional materials is to search for molecules with more π-extended systems [3-6]. It has been demonstrated that the extension of the TTF core not only leads to stabilized oxidized states and easy access to polycation states but also gives rise to an energetically narrower HOMO-LUMO gap [4]. Moreover, π-extended TTF units can enhance the dimensionality in materials by increasing intermolecular π…π and/or S…S interactions [5]. In this case, some TTF-based ligands and their metal complexes have been developed in the fields of redox-active sensors, multifunctional materials, and single-component molecular metals [6]. Tetrathiafulvalene with alkyl ligands have been widely studied owing to their interesting photophysical and redox properties, which make them useful in CO_2 remediation [7], solar energy systems [8], molecular electronics [9] and light switching devices [10]. By incorporation of alkyl ligands into TTF frameworks, it is possible to induce a substantial effect on the photochemical properties of the resulted metal complexes.
On the other hand, the development of organic NLO materials is of particular interest for their applications in frequency shifting, optical modulation, optical switching, optical logic, and optical memory for the emerging technologies in areas such as telecommunications, signal processing, and optical interconnections, etc [11-13]. In recent years, numerous experimental as well as theoretical (DFT) investigations have been performed for the electro-optic (EO) or non-linear optical (NLO) properties and other applications of organic molecules. Quantum chemical studies of simple models such as tetrathiafulvalene and its derivatives are the understanding of their electro-optic properties in terms of the influence of structural and solvent effects on such properties would be quite handy. So far, only scanty quantum chemical reports of the variation of dipole moments, polarizabilities of tetrathiafulvalene and its derivatives with geometry and solvents exist.
This work, therefore, derives from here and is an attempt to proffer theoretical explanations to the variation of the molecular dipole moments, polarizability, hyperpolarizability with the influence of frontier orbital energy, frequency dependent second order NLO property, atomic charge, molecular electrostatic potential surface and natural bond orbital analysis, reactivity descriptors, of (BDT-TTP) and its derivatives with molecular geometry.

2. Material and Methods
All computational calculations have been performed on personal computer using the Gaussian 09W program packages developed by Frisch and coworkers. The Becke's three parameter hybrid functional using the LYP correlation functional (B3LYP), one of the most robust functional of the hybrid family, was herein used for all the calculations, with 6-31G (d,p) basis set. Gaussian output files were visualized by means of GAUSSIAN VIEW 05 software.

3. Results and Discussion

3.1 Molecular Geometry

Before computing the frequencies and electronic properties, it is necessary to analyze the molecular structure of the compounds. So that the structures are optimized at DFT level of theory and numbering scheme is represented in Figure 1 and the calculated optimized geometrical parameters are presented in table 1-4. The geometry of the compounds under investigation is considered by possessing C_1 point group symmetry. The absence of imaginary frequencies confirmed that the stationary points correspond to minima on the Potential Energy Surface. The internal coordinates describe the position of the atoms in terms of distances, angles and dihedral angles with respect to an origin atom.

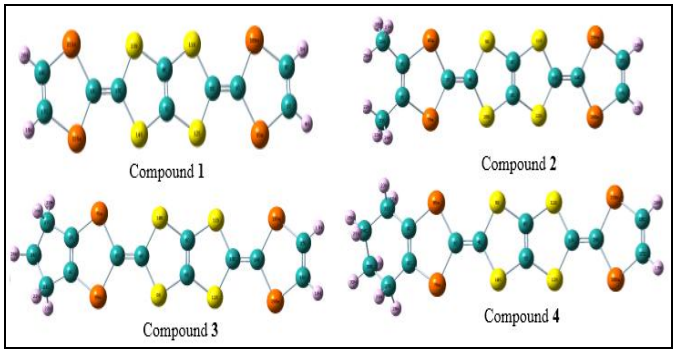

Fig 1: Optimized molecular structure of (BDT-TTP) and its derivatives 1-4

Table 1: Optimized geometric parameters of compound 1

Bond Length(Å)		Bond Angles (°)		Dihedral Angles (°)	
R(3,5)	***1.084***	A(6,1,9)	122.842	D(10,1,6,12)	180.000
R(3,10)	1.895	A(9,1,10)	114.316	D(6,1,9,2)	179.995
R(6,11)	1.794	A(3,2,4)	123.860	D(9,1,10,3)	0.005
R(8,11)	1.764	A(1,6,11)	122.583	D(1,6,11,8)	180.001
R(8,13)	1.764	A(11,6,12)	114.834	D(12,6,11,8)	0.001
R(15,16)	1.346	A(8,7,12)	118.460	D(14,7,12,6)	180.001
R(16,21)	1.914	A(12,7,14)	123.080	D(14,15,16,21)	180.000
R(18,21)	1.895	A(16,21,18)	93.089	D(12,7,8,13)	180.000
R(17,18)	1.334	A(7,8,11)	118.460	D(12,7,14,15)	180.001
R(18,20)	1.084	A(18,17,19)	123.860	D(14,7,8,11)	180.000
R(7,8)	1.342	A(7,14,15)	94.123	D(8,13,15,14)	0.001
R(6,12)	1.794	A(13,15,16)	122.583	D(3,2,9,1)	0.003
R(2,9)	1.895	A(18,17,19)	119.753	D(15,16,22,17)	179.995
R(1,6)	1.346	A(17,18,20)	123.860	D(22,17,18,20)	179.999
R(2,3)	1.334	A(14,15,16)	122.583	D(20,18,21,16)	179.997

Table 2: Optimized geometric parameters of compound 2

Bond Length(Å)		Bond Angles (°)		Dihedral Angles (°)	
R(1,4)	1.345	A(4,1,7)	123.211	D(7,1,4,9)	179.999
R(1,7)	1.906	A(7,1,8)	113.578	D(4,1,7,2)	179.996
R(2,3)	1.341	A(3,2,7)	118.834	D(7,2,3,25)	179.999
R(2,21)	1.503	A(3,2,21)	127.537	D(3,2,21,23)	120.462
R(4,9)	1.796	A(2,3,25)	127.537	D(7,2,21,24)	59.529
R(5,6)	1.342	A(1,4,9)	122.595	D(2,3,25,27)	120.472
R(5,12)	1.765	A(9,4,10)	114.810	D(1,4,9,6)	179.985
R(6,9)	1.764	A(6,5,12)	118.439	D(9,4,10,5)	0.017
R(12,13)	1.794	A(10,5,12)	123.068	D(12,5,6,9)	179.998
R(13,14)	1.346	A(5,12,13)	94.157	D(12,5,10,4)	179.992
R(14,19)	1.914	A(13,14,20)	122.846	D(10,5,12,13)	179.994
R(15,16)	1.334	A(17,15,20)	116.390	D(6,11,13,14)	179.996
R(16,18)	1.084	A(15,16,18)	123.855	D(11,13,14,20)	179.999
R(16,19)	1.895	A(14,20,15)	93.092	D(13,14,20,15)	180.000
R(21,22)	1.091	A(2,21,22)	111.899	D(20,15,16,18)	180.000

Table 3: Optimized geometric parameters of compound 3

Bond Length(Å)		Bond Angles (°)		Dihedral Angles (°)	
R(1,4)	1.346	A(4,1,7)	122.712	D(7,1,4,9)	178.643
R(1,7)	1.918	A(7,1,8)	114.574	D(4,1,7,2)	169.047
R(2,3)	1.339	A(3,2,7)	119.957	D(7,1,8,3)	11.509
R(2,7)	1.891	A(3,2,27)	112.499	D(7,2,3,21)	174.947
R(2,27)	1.507	A(8,3,21)	127.320	D(3,2,27,28)	106.117
R(4,10)	1.792	A(1,4,9)	123.190	D(7,2,27,24)	172.374
R(5,6)	1.344	A(9,4,10)	113.591	D(21,3,8,1)	178.724
R(5,10)	1.768	A(6,5,10)	117.901	D(1,4,9,6)	161.314
R(6,9)	1.768	A(6,5,12)	117.859	D(10,5,6,11)	179.879

R(12,13)	1.791	A(10,5,12)	124.241	D(12,5,10,4)	167.269
R(13,14)	1.346	A(6,11,13)	92.971	D(6,11,13,14)	160.809
R(14,19)	1.910	A(11,13,14)	123.181	D(11,13,14,20)	178.427
R(15,17)	1.084	A(13,14,19)	123.013	D(13,14,20,15)	167.105
R(24,26)	1.093	A(18,16,19)	116.579	D(20,15,16,18)	178.633
R(24,27)	1.556	A(22,21,24)	112.011	D(18,16,19,14)	172.534

Table 4: Optimized geometric parameters of compound 4

Bond Length(Å)		**Bond Angles (°)**		**Dihedral Angles (°)**	
R(1,4)	1.346	A(7,1,8)	113.533	D(8,1,4,10)	178.206
R(1,7)	1.907	A(3,2,7)	118.853	D(4,1,8,3)	167.329
R(2,3)	1.339	A(3,2,27)	123.892	D(27,2,3,8)	178.769
R(2,7)	1.913	A(7,2,27)	117.227	D(27,2,7,1)	172.468
R(2,27)	1.509	A(2,3,8)	119.015	D(3,2,27,29)	136.484
R(4,9)	1.792	A(2,3,21)	123.829	D(1,4,10,5)	160.989
R(5,6)	1.344	A(1,4,9)	123.174	D(12,5,6,9)	179.999
R(6,11)	1.769	A(9,4,10)	113.569	D(11,6,9,4)	167.181
R(11,13)	1.791	A(5,6,11)	117.858	D(9,6,11,13)	167.269
R(13,14)	1.346	A(9,6,11)	124.251	D(5,12,13,14)	160.876
R(14,19)	1.910	A(6,11,13)	92.991	D(12,13,14,19)	178.461
R(16,18)	1.084	A(15,16,19)	119.463	D(13,14,19,16)	166.975
R(16,19)	1.900	A(22,21,23)	106.038	D(17,15,16,19)	178.628
R(24,30)	1.533	A(7,1,8)	113.533	D(17,15,20,14)	172.469
R(27,30)	1.538	A(3,2,7)	118.853	D(25,24,30,31)	179.827

3.2 Molecular Electrostatic Potential

MESP has been established extensively as a useful quantity to explain hydrogen bonding, reactivity, structure activity of molecular behaviors and charge distributions of molecules, which are used to visualize variably charged regions of a molecule. The molecular electrostatic potential is related to the electron density and a very useful descriptor for determining sites for electrophilic attack and nucleophilic reactions as well as hydrogen-bonding interactions [14-16]. Negative electrostatic potential corresponds to the area, in which the proton is attracted by concentrated electron density in the molecule (lone pairs, π bonding). The positive electrostatic potential corresponds to the area, in which the proton is repelled by atomic nuclei. The different values of the electrostatic potential at the surface are shown by various colors: blue indicates the strongest attraction, while the red indicates the strongest repulsion. Potential decreases in the order blue > green > yellow >orange > red. As can be seen from the MESP map of the title molecules (Figure 2), suggested that the potential spreads widely between hydrogen atoms of alkyl groups (blue) and skeleton of tetrathiapentalene (red).

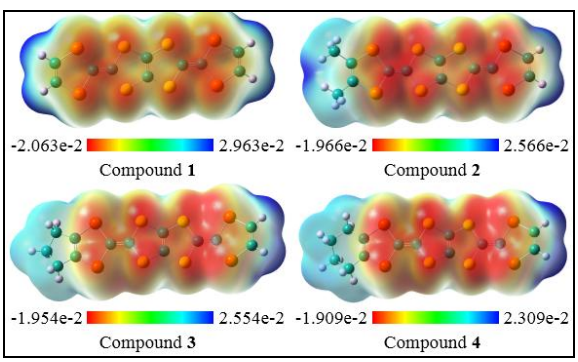

Fig 2: Molecular electrostatic potential surface of (BDT-TTP) and its derivatives 1-4

3.3 Frontier Molecular Orbitals (FMOs)

Molecular orbitals (MO's) both the Highest Occupied Molecular Orbital (HOMO) and Lowest Unoccupied Molecular Orbital (LUMO) and their energy gap (ΔE) are very useful parameters for quantum chemistry. We can determine the way the molecule interacts with other species; hence, they are called the Frontier molecular orbitals (FMO's). HOMO, which can be thought the outermost orbital containing electrons, tends to act as electron donor. On the other hand, LUMO can be thought the innermost orbital containing free places to accept electrons. To explain several types of reactions and for predicting the most reactive position in conjugated systems, molecular orbital and their properties are used. A molecule having a small frontier orbital gap is more polarizable and is generally associated with a high chemical reactivity and low kinetic stability [17]. This is also used by the frontier electron density for predicting the most reactive position in π-electron systems and also explains several types of reaction in conjugated system [18]. The conjugated molecules are characterized by a small energy gap, which result a significant degree of intra-molecular charge transfer (ICT) from the end-gapping electron-donor groups to the efficient electron acceptor group through π-conjugated path [19]. Surfaces for the frontier orbitals are drawn to understand the bonding scheme of present compounds. The energy is a critical parameter in determining molecular electrical transport properties because it is a measure of electron conductivity. The plots of MO's of the highest occupied molecular orbital HOMO and LUMO) for compound 2 are shown in Figure 3. All the HOMO and the lowest unoccupied molecular orbital LUMO have nodes. The nodes in each HOMO and LUMO are placed symmetrically. The positive phase is red and the negative is green. To understand the bonding features of the title molecules, tow important molecular orbitals (MO) were examined for the title compounds.

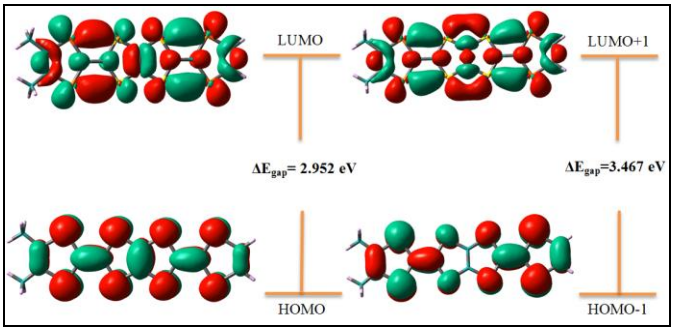

Fig 3: HOMO-LUMO Structure with the energy level diagram of compound 2

3.4. Global Reactivity Descriptors

DFT based reactivity descriptors have been extensively used for rationalization and interpretation of diverse aspects of chemical bonding, reaction mechanism, and reactive centers. These quantum chemical descriptors are related to electronic structure of compounds and to the mechanism that is involved in the covalent bond formation as a result of reaction between the nucleophiles and the electrophiles. The chemical reactivity and site selectivity of the molecular systems have been determined on the basis of Koopman's theorem [20]. Energies of frontier molecular orbitals (E_{HOMO}, E_{LUMO}), have been used to calculate global reactivity descriptors such as, electronegativity (χ), chemical potential (μ), Global hardness (η), global softness (S), and electrophilicity index (ω). These important descriptors are calculated as follows:

Electronegativity (χ) = -1/2(E_{LUMO} + E_{HOMO}), chemical potential (μ) = 1/2 (E_{LUMO} + E_{HOMO}), global hardness (η) = 1/2 (E_{LUMO} –E_{HOMO}), global softness (S) = 1/2 η and electrophilicity index (ω) = $\mu^2/2\eta$. The energies of frontier molecular orbitals (E_{HOMO}, E_{LUMO}), energy gap (E_{LUMO} – E_{HOMO}), electronegativity (χ), chemical potential (μ), global hardness (η), global softness (S), global electrophilicity index (ω) for compounds 1-4 are given in Table 5. Larger HOMO-LUMO energy gap describes greater hardness of the molecule. Larger HOMO-LUMO energy gap as well as hardness for compounds 3 and 4 (E_{LUMO} –E_{HOMO} = 3.260, η = 1.630), (E_{LUMO} –E_{HOMO} = 3.255, η = 1.627) respectively, as compared to compound 1 (E_{LUMO} –E_{HOMO} = 2.979, η = 1.490) suggest that compound 2 is more reactive than compound 1, 3 and 4. Further, from the Table 5 it can be seen that higher value of global electrophilicity index for compound 1, suggest that it is more electrophilic than compound 2, 3 and 4.

Table 5: Quantum chemical descriptors of (BDT-TTP) and its derivatives 1-4

Parameters	Compound 1	Compound 2	Compound 3	Compound 4
E_{HOMO} (eV)	-4.563	-4.480	-4.636	-4.623
E_{LUMO} (eV)	-1.584	-1.528	-1.376	-1.368
ΔE_{gap} (eV)	2.979	2.952	3.260	3.255
IE (eV)	4.563	4.480	4.636	4.623
EA (eV)	1.584	1.528	1.376	1.368
μ (eV)	-3.073	-3.004	-3.006	-2.996
χ (eV)	3.073	3.004	3.006	2.996
η (eV)	1.490	1.476	1.630	1.627
S (eV)	0.336	0.339	0.307	0.307
ω (eV)	3.171	3.057	2.771	2.757

3.5 Local Reactivity Descriptors

To determine the reactive site/s within the molecule, local reactivity descriptors such as Fukui Function (FF) is used. Using Hirschfeld atomic charges of neutral, cation and anion state of compounds **1-4**, the condensed Fukui functions (f_k^+, f_k^-, f_k^0) have been calculated.

Fukui functions are calculated by following equation.

$f^+ = [q(N+1) - q(N)]$, for nucleophilic attack,

$f^- = [q(N) - q(N-1)]$, for electrophilic attack,

$f^0 = [q(N+1) - q(N-1)]/2$, for radical attack.

where, q is the gross charge of atom k in the molecule and N, N+1, N-1 are electron systems containing neutral, anion, cation form of molecule respectively. Where +, -, 0 signs show nucleophilic, electrophilic and radical attacks respectively. Fukui functions for selected atomic sites in compounds 1-4 are shown in Tables 6 and 7.

Table 6: Order of the reactive sites on compounds 1 and 2

Compound 1					Compound 2				
Atom	6 C	15 C	1 C	16 C	Atom	13 C	4 C	1 C	14 C
f^+	0,018	0,018	0,017	0,017	f^+	0.028	0.027	0.018	0.013
Atom	15 C	6 C	7 C	8 C	Atom	13 C	4 C	2 C	3 C
f^-	0.019	0.019	0.000	0.000	f^-	0.020	0.016	0.003	0.003
Atom	6 C	15 C	1 C	16 C	Atom	13 C	4 C	1 C	14 C
f^0	0.018	0.018	0.006	0.006	f^0	0.024	0.022	0.006	0.003

Table 7: Order of the reactive sites on compounds 3 and 4

Compound 3					Compound 4				
Atom	4 C	13 C	14 C	2 C	Atom	13 C	4 C	1 C	14 C
f^+	0.026	0.026	0.005	0.004	f^+	0.024	0.023	0.004	0.001
Atom	13 C	4 C	5 C	6 C	Atom	13 C	4 C	6 C	5 C
f^-	0.024	0.017	0.009	0.009	f^-	0.024	0.019	0.008	0.008
Atom	13 C	4 C	14 C	2 C	Atom	13 C	4 C	1 C	14 C
f^0	0.025	0.021	0.006	0.004	f^0	0.024	0.021	0.005	0.004

In this study, gross charges were calculated by using Mulliken charge analysis in order to calculate the condensed Fukui functions. The condensed Fukui functions for the compounds are given in Table 6 and 7. These tables show that the most reactive site of compounds 1, 2, 3 and 4 are the 6C, 13C, 4C and 13C respectively, for the nucleophilic attack and for the electrophilic attack are 15C for compound 1 and 13C for compounds 2, 3 and 4 and for the radical attack, 6C in compound 1 and 13C in compounds 2, 3 and 4.

3.6. Natural Bond Orbital Analysis (NBO)

NBO calculations have been performed using Gaussian 09W package program [21] at the B3LYP/6-31G(d,p) levels in order to understand various second-order interactions between the filled orbitals of one subsystem and vacant orbitals of another subsystem, which are a measure of the intermolecular delocalization or hyperconjugation. A useful aspect of the NBO method is that it gives information about interactions in both filled and virtual orbital spaces, which could enhance the analysis of intra and intermolecular interactions. NBO method makes possible to examine hyperconjugative interactions due to electron transfers from filled bonding orbitals (donor) to empty anti-bonding orbitals (acceptor) [22, 23]. The second-

order Fock matrix was used to evaluate the donor–acceptor interactions in the NBO basis [24]. The interactions result in a loss of occupancy from the localized NBO of the idealized Lewis structure into an empty non-Lewis orbital. For each donor (i) and acceptor (j), the stabilization energy E associated with the delocalization $i \rightarrow j$ is estimated [25]. The natural bond orbital (NBO) [26] second order perturbation stabilization energy (E) was defined. Hybrids of natural bond orbitals calculated by NBO analysis are given in Tables 8-11 for the title compounds.

Table 8: Second order perturbation theory analysis of Fock matrix on NBO of compound 1

Donor(i)	ED/e	Acceptor (j)	ED/e	E(2) Kcal/mol	E(j)-E(i) a.u	F(i.j) a.u
LP(2) S11	1.80207	π*(C7-C8)	0.38069	21.17	0.24	0.066
LP(2) S12	1.80207	π*(C7-C8)	0.38069	21.17	0.24	0.066
LP(2) S13	1.80207	π*(C7-C8)	0.38069	21.17	0.24	0.066
LP(2) S14	1.80207	π*(C7-C8)	0.38069	21.17	0.24	0.066
LP(2) S11	1.80207	π*(C1-C6)	0.40088	18.71	0.24	0.063
LP(2) S13	1.80207	π*(C15-C16)	0.40088	18.71	0.24	0.063
LP(2) Se9	1.79632	π*(C2-C3)	0.20062	18.45	0.24	0.060
LP(2) Se21	1.79632	π*(C17-C18)	0.20062	18.45	0.24	0.060
LP(2) Se 9	1.79632	π*(C1-C6)	0.40088	17.24	0.22	0.058
LP(2) Se21	1.79632	π*(C15-C16)	0.40088	17.24	0.22	0.058
σ(C1-Se9)	1.96803	σ*(C6 -S11)	0.04209	6.04	0.77	0.061
σ(C1-Se10)	1.96803	σ*(C6 -S12)	0.04209	6.04	0.77	0.061
σ(C16-Se 21)	1.96803	σ*(S14 -C15)	0.04209	6.04	0.77	0.061
σ(C16 -Se 22)	1.96803	σ*(S13-C15)	0.04209	6.04	0.77	0.061
σ(C2-H4)	1.97466	σ*(C3-Se10)	0.02377	5.99	0.69	0.058
σ(C 3-H5)	1.97466	σ*(C2 -Se9)	0.02377	5.99	0.69	0.058
σ(C17-H19)	1.97466	σ*(C18-Se21)	0.02377	5.99	0.69	0.058
σ(C6-S11)	1.96823	σ*(C1-Se9)	0.03917	4.89	0.76	0.055
σ(S13-C15)	1.96823	σ*(C16 -Se22)	0.03917	4.89	0.76	0.055
σ(C7-S12)	1.97360	σ*(C8-S13)	0.02840	4.57	0.86	0.056

Table 9: Second order perturbation theory analysis of Fock matrix on NBO of compound 2

Donor(i)	ED/e	Acceptor(j)	ED/e	E(2) Kcal/mol	E(j)-E(i) a.u	F(i.j) a.u
LP(2) S9	1.80318	π*(C5-C6)	0.38071	21.24	0.24	0.066
LP(2) S11	1.80222	π*(C5-C6)	0.38071	21.07	0.24	0.066
LP(2) S11	1.80222	π*(C13-C14)	0.40097	18.78	0.24	0.063
LP(2) S12	1.80222	π*(C13-C14)	0.40097	18.78	0.24	0.063
LP(2) Se19	1.79677	π*(C15-C16)	0.20088	18.47	0.24	0.060
LP(2) Se20	1.79677	π*(C15-C16)	0.20088	18.47	0.24	0.060
LP(2) S9	1.80318	π*(C1-C4)	0.39773	18.45	0.24	0.063
LP(2) S10	1.80318	π*(C1-C4)	0.39773	18.45	0.24	0.063
LP(2) Se7	1.81216	π*(C1-C4)	0.39773	17.67	0.22	0.059
LP(2) Se19	1.79677	π*(C13-C14)	0.40097	17.17	0.22	0.058
LP(2) Se7	1.81216	π*(C2-C3)	0.21731	16.18	0.26	0.058
σ(C1-Se7)	1.96801	σ*(C4 -S9)	0.04270	6.02	0.77	0.061
σ(C1 -Se8)	1.96801	σ*(C4 -S10)	0.04270	6.02	0.77	0.061
σ(C14 -Se19)	1.96809	σ*(S12-C13)	0.04205	6.02	0.77	0.061
σ(C15-H17)	1.97469	σ*(C16-Se19)	0.02378	5.98	0.69	0.058
σ(C16-H18)	1.97469	σ*(C15-Se20)	0.02378	5.98	0.69	0.058
σ(C2 -Se7)	1.96657	σ*(C3-C25)	0.01823	5.57	0.99	0.067
σ(C2-C21)	1.97827	σ*(C2-C3)	0.02725	5.20	1.30	0.074
σ(C4-S10)	1.96831	σ*(C1-Se8)	0.03615	4.91	0.77	0.055
σ(S12-C13)	1.96830	σ*(C14-Se19)	0.03923	4.90	0.76	0.055

Table 10: Second order perturbation theory analysis of Fock matrix on NBO of compound 3

Donor(i)	ED/e	Acceptor(j)	ED/e	E(2) Kcal/mol	E(j)-E(i) a.u	F(i.j) a.u
LP(2) S9	1.80249	π*(C5-C6)	0.37206	20.18	0.24	0.065
LP(2) S10	1.80249	π*(C5-C6)	0.37206	20.18	0.24	0.065
LP(2) S11	1.80089	π*(C5-C6)	0.37206	20.16	0.24	0.065
LP(2) S12	1.80089	π*(C5-C6)	0.37206	20.16	0.24	0.065
LP(2) Se7	1.79808	π*(C2-C3)	0.22651	17.77	0.26	0.061
LP(2) Se8	1.79808	π*(C2-C3)	0.22651	17.77	0.26	0.061
LP(2) Se19	1.79160	π*(C15-C16)	0.19489	17.48	0.25	0.059

LP(2) Se20	1.79160	π*(C15-C16)	0.19489	17.48	0.25	0.059
LP(2) Se19	1.79160	π*(C13-C14)	0.36361	13.69	0.24	0.054
LP(2) Se20	1.79160	π*(C13-C14)	0.36361	13.69	0.24	0.054
LP(2) S11	1.80089	π*(C13-C14)	0.36361	13.16	0.26	0.055
LP(2) S12	1.80089	π*(C13-C14)	0.36361	13.16	0.26	0.055
LP(2) S9	1.80249	π*(C1-C4)	0.36110	13.15	0.26	0.055
LP(2) S10	1.80249	π*(C1-C4)	0.36110	13.15	0.26	0.055
σ(C1-Se7)	1.96665	σ*(C4-S9)	0.04577	6.10	0.77	0.061
σ(C1-Se 8)	1.96665	σ*(C4-S10)	0.04577	6.10	0.77	0.061
σ(C2-C27)	1.97357	σ*(C3-Se8)	0.03649	6.04	0.77	0.061
σ(C3-C21)	1.97357	σ*(C2 -Se7)	0.03649	6.04	0.77	0.061
σ(C14-Se19)	1.96836	σ*(S12-C13)	0.04593	5.99	0.77	0.061
σ(C15-H17)	1.97498	σ*(C16 -Se19)	0.02860	5.94	0.69	0.057

Table 11: Second order perturbation theory analysis of Fock matrix on NBO of compound 4

Donor(i)	ED/e	Acceptor(j)	ED/e	E(2) Kcal/mol	E(j)-E(i) a.u	F(i.j) a.u
LP(2) S9	1.80166	π*(C5-C6)	0.37204	20.24	0.24	0.065
LP(2) S10	1.80169	π*(C5-C6)	0.37204	20.24	0.24	0.065
LP(2) S11	1.80082	π*(C5-C6)	0.37204	20.10	0.24	0.065
LP(2) S12	1.80084	π*(C5-C6)	0.37204	20.10	0.24	0.065
LP(2) Se19	1.79193	π*(C15-C16)	0.19492	17.48	0.25	0.059
LP(2) Se20	1.79192	π*(C15-C16)	0.19492	17.47	0.25	0.059
LP(2) Se8	1.80344	π*(C2-C3)	0.21759	16.37	0.26	0.059
LP(2) Se7	1.80409	π*(C2 -C3)	0.21759	16.20	0.26	0.058
LP(2) Se7	1.80409	π*(C1-C4)	0.36152	14.02	0.24	0.054
LP(2) Se8	1.80344	π*(C1-C4)	0.36152	14.00	0.24	0.054
LP(2) Se19	1.79193	π*(C13-C14)	0.36352	13.64	0.24	0.054
LP(2) Se20	1.79192	π*(C13-C14)	0.36352	13.64	0.24	0.054
LP(2) S11	1.80082	π*(C13-C14)	0.36352	13.20	0.26	0.055
LP(2) S12	1.80084	π*(C13-C14)	0.36352	13.20	0.26	0.055
LP(2) S10	1.80169	π*(C1-C4)	0.36152	13.07	0.26	0.055
LP(2) S9	1.80166	π*(C1-C4)	0.36152	13.06	0.26	0.055
σ(C1-Se8)	1.96790	σ*(C4 -S10)	0.04651	6.03	0.77	0.061
σ(C1-Se7)	1.96795	σ*(C4-S9)	0.04652	6.01	0.77	0.061
σ(C14-Se19)	1.96837	σ*(S12-C13)	0.04593	5.98	0.77	0.061
σ(C14-Se20)	1.96838	σ*(S11-C13)	0.04592	5.98	0.77	0.061

The intra molecular interaction for the title compounds is formed by the orbital overlap between: σ(C1-Se9) and σ*(C6-S11) for compound 1, σ(C1-Se7) and σ*(C4-S9) for compound 2, σ(C1-Se7)and σ*(C4-S9) for compound 3, σ(C1-Se8) and σ*(C4 -S10) for compound 4 respectively, which result into intermolecular charge transfer (ICT) causing stabilization of the system. The intra molecular hyper conjugative interactions of σ(C1-Se9) to σ*(C6 -S11) for compound 1, σ(C1-Se7) to σ*(C4-S9) for compound 2, σ(C1-Se7) to σ*(C4-S9) for compound 3 and σ(C1-Se8) to σ*(C4 -S10) for compound 4 lead to highest stabilization of 6.04, 6.02, 6.10 and 6.03 kJ mol^{-1} respectively. In case of LP(2)S11orbital to the π*(C7-C8) for compound 1, LP(2)S9 orbital to π*(C5-C6) for compound 2, LP(2)S9 orbital to π*(C5-C6) for compound 3 and LP(2)S9 orbital to π*(C5-C6) for compound 4 respectively, show the stabilization energy of 21.17, 21.24, 20.18 and 20.24 kJ mol^{-1} respectively.

3.7. Nonlinear Optical Properties (NLO)

Many organic molecules that contain conjugated electrons have characterized hyperpolarizabilities which can be analyzed by vibrational spectroscopy. It is observed that, the intramolecular charge transfer from the donor to the acceptor group through a single double-bond conjugated path can induce large variations of both the molecular dipole moment and the molecular polarizability. Nonlinear optics deals with the interaction of applied electromagnetic fields in various materials to generate new electromagnetic fields, altered in wavenumber, phase, or other physical properties. Organic molecules able to manipulate photonic signals efficiently are of importance in technologies such as optical communication, optical computing, and dynamic image processing [27]. However, The NLO activity give the key functions for frequency shifting, optical modulation, optical switching and optical logic for the developing technologies in areas such as communication, signal processing and optical interconnections [28]. Hyperpolarizabilities are very sensitive to basis sets and levels of theoretical computations employed that the electron correlation can change the value of hyperpolarizability. In this context, the dynamic first hyperpolarizability of the title compounds is also calculated in the present study. The dipole moment (μ), polarizability (α) and first order hyperpolarizability (β_0) are calculated using DFT/6-31G (d,p). The complete equations for calculating their magnitudes using the (x, y, z) components obtained from Gaussian 09 are taken from. It is well known that the higher values of dipole moment, molecular polarizability and first order hyperpolarizability are important for more active NLO

properties.

In the present study, the first hyperpolarizability (β_0), converged mean polarizability (α), anisotropic polarizability ($\Delta\alpha$) and molecular dipole moment (μ) (Debye) of this novel molecular system are calculated using DFT/6-31G (d,p) basis set, based on the finite field approach. In the presence of an applied electric field, the energy of a system is a function of the electric field. The first hyperpolarizability is a third-rank tensor that can be described by a 3 × 3 × 3 matrix. The 27 components of the 3D matrix can be reduced to 10 components because of the Kleinman symmetry [29]. The calculated dipole moments are also quite large for these systems. The large dipole moments suggest a significant contribution from resonance and are consistent with significant push pull effects. In Table 12, results using the B3LYP methods with the 6-31G(d,p) basis set are listed for (BDT-TTP) and its derivatives 1-4 for the following parameters: first-order hyperpolarizability (β), converged mean polarizability (α), anisotropic polarizability (Δα) and molecular dipole moment (μ) (Debye). The calculated first hyperpolarizability is about ~10 times greater than that of urea. The above results show that title compounds is best material for NLO applications. We conclude that the title compounds are an attractive object for future studies of nonlinear optical properties. The changes made by substitutions on the rings estimate an extended π-electron delocalization over the TTF molecules, which is responsible for the non-linearity of the molecules.

Table 12. The dipole moments μ (D), polarizability α, the average polarizability α (esu), the anisotropy of the polarizability Δα (esu), and the first hyperpolarizability β (esu) of (BDT-TTP) and its derivatives 1-4 calculated by B3LYP/6-31G(d,p) method.

Parameters	Compound 1	Compound 2	Compound 3	Compound 4
β_{xxx}	89.3608	-147.1828	-148.9244	-101.5918
B_{yyy}	-2.3332	1.5827	-0.4758	0.0833
B_{zzz}	0.5027	2.4147	-1.3950	-4.8758
B_{xyy}	-0.5811	17.6863	3.3468	-31.8896
B_{xxy}	-38.7369	6.2484	-33.1352	-0.1108
B_{xxz}	3.7906	-2.5458	27.1669	-9.1822
B_{xzz}	-22.4931	8.9055	6.7711	-16.9062
B_{yzz}	-2.3639	-3.8876	0.9251	0.2271
B_{yyz}	3.1657	3.5499	1.0603	-2.6133
B_{xyz}	-2.5582	8.9900	-16.4806	0.2309
B_{tot}(esu)x10^{-33}	168.8291	182.8418	144.1900	80.7088
μ_x	-1.7750	0.6850	-0.3682	1.4065
μ_y	0.1315	-0.7675	-0.3768	-0.0008
μ_z	0.5833	0.2499	0.0555	0.3360
μ_{tot}(D)	1.8731	1.0586	0.5298	1.4461
α_{xx}	-97.3608	-111.1080	-114.7304	-140.2106
α_{yy}	-122.9225	-134.2826	-134.5315	-199.5114
α_{zz}	-127.6286	-143.5612	-143.7162	-211.8323
α_{xy}	-5.8857	-0.5837	5.4723	-0.0989
α_{xz}	0.1706	-6.4007	-5.3997	9.8948
α_{yz}	0.5409	0.9099	-3.0989	0.0858
α_0(esu)x10^{-24}	30.0122	31.0579	29.4011	68.5040
$\Delta\alpha$(esu)x10^{-24}	4.4478	4.6028	4.3573	10.1523

Since the values of the polarizabilities (Δα) and the hyperpolarizabilities (β_{tot}) of the GAUSSIAN 09 output are obtained in atomic units (a.u.), the calculated values have been converted into electrostatic units (e.s.u.) (for α; 1 a.u = 0.1482 x 10^{-24} e.s.u., for β; 1 a.u = 8.6393 x 10^{-33} e.s.u.). The calculated values of dipole moment (μ) for the title compounds were found to be 1.8731, 1.0586, 0.5298 and 1.4461 D respectively, which are approximately one times than to the value for urea (μ = 1.3732 D). Urea is one of the prototypical molecules used in the study of the NLO properties of molecular systems. Therefore, it has been used frequently as a threshold value for comparative purposes. The calculated values of polarizability are 30.0122 x 10^{-24}, 31.0579 x 10^{-24}, 29.4011 x 10^{-24} and 68.5040 x 10^{-24} esu respectively; the values of anisotropy of the polarizability are 4.4478, 4.6028, 4.3573 and 10.1523 esu, respectively. The magnitude of the molecular hyperpolarizability (β) is one of important key factors in a NLO system. The DFT/6-31G(d,p) calculated first hyperpolarizability value (β) of bis(dithiol-ylidene)-tetrathiapentalene molecules are equal to 168.8291 x 10^{-33}, 182.8418 x 10^{-33}, 144.1900 x 10^{-33} and 80.7088 x 10^{-33} esu. The first hyperpolarizability of title molecules is approximately 0.49, 0.53, 0.42 and 0.23 times than those of urea (β of urea is 343.272 x10^{-33} esu obtained by B3LYP/6-311G (d,p) method). This result indicates that (BDT-TTP) and its derivatives 1-4 are not nonlinear.

4. Conclusion

This paper reports a comprehensive computational structural study of series of (BDT-TTP) and its derivatives 1-4. A number of reactivity parameters have been done by employing density functional theory (DFT) with 6-31G(d,p) as the basis sets. Reactivity reflects the susceptibility of the title compounds towards a specific chemical reaction and plays a key role in, for example, the design of new molecules and understanding material science. The chemical reactivity of molecules shows that compound 2 is more polarizable and is associated with a high chemical reactivity, low kinetic stability and is also termed as soft molecule. The results reported in the present paper can help in the experimental investigations on the origin of the design of new molecules in the field of organic materials.

5. Acknowledgments

This work was generously supported by the (General Directorate for Scientific Research and Technological Development, DGRS-DT) and Algerian Ministry of Scientific Research.

6. References

1. Coronado E, Day P. Magnetic molecular conductors. Chem. Rev. 2004; 104(11):5419-5448.
2. Dumur F, Gautier N, Gallego-Planas N, Sahin Y, Levillain E, Mercier N, *et al*. novel fused D-A dyad and A-D-A triad incorporating tetrathiafulvalene and *p*-benzoquinone. J Org, Chem. 2004; 69(6): 2164-2177.
3. Bendikov M, Wudl F, Perepichka DF. Tetrathiafulvalenes, oligoacenenes, and their buckminsterfullerene derivatives: The brick and mortar of organic electronics. Chem. Rev. 2004; 104(11):4891-4946.

4. Frère P, Skabara P. Salts of extended tetrathiafulvalene analogues: relationships between molecular structure, electrochemical properties and solid state organisation. Chem. Soc. Rev. 2005; 34(1):69-98.
5. Jia HP, Liu SX, Sanguinet L, Levillain E, Decurtins S. Star-shaped tetrathiafulvalene-fused coronene with large pi-extended conjugation. J Org, Chem. 2009; 74(15):5727-5729.
6. Lorcy D, Bellec N, Fourmigué M, Avarvari N. Tetrathiafulvalene-based group XV ligands: Synthesis, coordination chemistry and radical cation salts. Coord. Chem. Rev. 2009; 253:1398-1438.
7. Takeda H, Ishitani O. Development of efficient photocatalytic systems for CO2 reduction using mononuclear and multinuclear metal complexes based on mechanistic studies. Coord. Chem. Rev. 2010; 254(3-4):346-354.
8. Moser JE, Bonnôte P, Grätzel M. Molecular photovoltaics. Coord. Chem. Rev. 1998; 171:245-250.
9. Balzani V, Gómez-López M, Stoddart JF. Molecular machines. Acc. Chem. Res. 1998; 31(7): 405–414.
10. Liu Y, Chouai A, Degtyareva NN, Lutterman DA, Dunbar KR, Turro C. Chemical control of the DNA light switch: cycling the switch ON and OFF. J. Am. Chem. Soc. 2005; 127(31):10796-10797.
11. Geskin VM, Lambert C, Bredas JL. Origin of high second- and third-order nonlinear optical response in ammonio / borato diphenylpolyene zwitterions: the remarkable role of polarized aromatic groups. J Am. Chem. Soc. 2003; 125(50):15651–15658.
12. Sajan D, Joe H, Jayakumar VS, Zaleski J. Structural and electronic contributions to hyperpolarizability in methyl p-hydroxy benzoate. J Mol. Struct. 2006; 785(1-3):43-53.
13. Bella SD, Fragala I, Ledoux I, Diaz-Garcia MA, Lacroix PG, Marks TJ. Sizable Second-order nonlinear optical response of donor-acceptor bis salicylaldiminato nickel (II) schiff base complexes. Chem. Mater. 1994; 6(7):881-883.
14. Luque FJ, Lopez JM, Orozco M. Perspective on Electrostatic interactions of a solute with a continuum. A direct utilization of ab initio molecular potentials for the prevision of solvent effects. Theor. Chem. Acc. 2000; 103:343-345.
15. Okulik N, Jubert AH. Theoretical analysis of the reactive sites of non-steroidal anti–inflammatory drugs. Internet Electron. J Mol. Des. 2005; 4(1):17-30.
16. Parlak C, Akdogan M, Yildirim G, Karagoz N, Budak E, Terzioglu C. Density functional theory study on the identification of 3-[(2-morpholinoethylimino) methyl] benzene-1,2-diol. Spectrochim. Acta A. 2011; 79(1):263-271.
17. Lewis DFV, Loannides C, Parke DV. Interaction of a series of nitriles with the alcohol-inducible isoform of P450: computer analysis of structure-activity relationships. Xenobiotica. 1994; 24(5):401-408.
18. Fukui K, Yonezawa T, Shingu H. A molecular orbital theory of reactivity in aromatic hydrocarbons. J Chem. Phys. 1952; 20(4):722-725.
19. Cho LH, Kerterz M. Conformational information from vibrational spectra of styrene, trans-Stilbene, and cis-Stilbene. J Phys. Chem. A. 1997; 101(20):3823-3831.
20. Parr RG, Yang W. Density functional theory of atoms and molecules, Oxford University Press, Oxford, New York, 1989.
21. Frisch MJ, Trucks GW, Schlegel HB, Scuseria GE, Robb MA, Cheeseman JR. Gaussian 09, Revision A.1, Gaussian Inc, Wallingford CT, 2009.
22. Pir H, Günay N, Tamer Ö, Avcı D, Atalay Y. Theoretical investigation of 5-(2-acetoxyethyl)-6-methylpyrimidin-2,4-dione: conformational study, NBO and NLO analysis, molecular structure and NMR spectra. Spectrochim. Acta A. 2013; 112:331-342.
23. Pir H, Günay N, Tamer Ö, Avcı D, Tarcan E, Atalay Y. Quantum chemical computational studies on bis-thiourea zinc acetate. Mater. Sci-Pol. 2013; 31(3):357-371.
24. Chocholousova J, Spirko V, Hobza P. First local minimum of the formic acid dimer exhibits simultaneously red-shifted O–H···O and improper blue-shifted C–H···O hydrogen bonds. Phys. Chem. Chem. Phys. 2004; 6:37-41.
25. Pir H, Gunay N, Avcı D, Atalay Y. Molecular structure, vibrational spectra, NLO and NBO analysis of bis (8-oxy-1-methylquinolinium) hydroiodide. Spectrochim. Acta A. 2012; 96:916-924.
26. Fukui K. Role of frontier orbitals in chemical reactions. Science. 1982; 218:747-54.
27. Ge YQ, Xia Y, Wei F, Dong WL, Zhao BX. N-Benzyl-5-phenyl-1H-pyrazole-3-carboxamide. Acta. Cryst. 2007; E63:1186-1187.
28. Andraud C, Brotin T, Garcia C, Pelle F, Goldner P, Bigot B, Collet A. Theoretical and experimental investigations of the nonlinear optical properties of vanillin, polyenovanillin, and bisvanillin derivatives. J Am. Chem. Soc. 1994; 116(5):2094-2102.
29. Kleinman DA. Nonlinear dielectric polarization in optical media. Phys. Rev. 1962; 126(6):1977-1979.